Induced Drag Calculations in the Unsteady Vortex Lattice Method

Robert J. S. Simpson* and Rafael Palacios†

Imperial College, London, SW7 2AZ, United Kingdom

and

Joseba Murua‡

University of Surrey, Guildford, GU2 7XH, United Kingdom

Nomenclature

α	angle of attack, rad
Γ	circulation, $m^2 s^{-1}$
λ	wake wavelength, m
ρ_∞	free-stream air density, kgm^{-3}
$\boldsymbol{\tau}$	panel tangential vector
ω	angular velocity, $rad\, s^{-1}$
a	non-dimensional distance between aerofoil mid-chord and centre of rotation
A	panel area, m^2
b	semi-chord, m
Δb	panel span, m
B	wingspan, m
c	aerofoil chord, m
Δc	panel chord, m
C	Theodorsen's function, $C(k) = F(k) + iG(k)$
C_d	sectional drag coefficient
C_D	wing drag coefficient
C_l	sectional lift coefficient
C_s	sectional leading-edge suction coefficient

*Graduate Student, Department of Aeronautics. AIAA Student Member.

†Senior Lecturer, Department of Aeronautics. E-mail: rpalacio@imperial.ac.uk. AIAA Member.

‡Lecturer, Department of Mechanical Engineering Sciences. AIAA Member.

d sectional drag, Nm^{-1}

D panel drag contribution, N

$\mathbf{F}$ force vector, N

h plunge displacement, m

k reduced frequency

l sectional lift, Nm^{-1}

$\mathbf{l}$ vortex segment vector, m

L panel lift contribution, N

M number of chordwise panels

$\mathbf{n}$ panel normal vector

N number of spanwise panels

P orthogonal projection operator

s reduced time

S leading-edge suction term, $m^{3/2}s^{-1}$

Δt time step, s

$\mathbf{U}$ velocity vector, ms^{-1}

U_∞ free-stream velocity, ms^{-1}

Subscript

i panel index in the chordwise direction

j panel index in the spanwise direction

Superscript

$(\dot{\bullet})$ time derivative

$(\hat{\bullet})$ unit vector

$(\bar{\bullet})$ amplitude

I. Introduction

The Unsteady Vortex Lattice Method (UVLM) solves unsteady, potential flows around thin lifting surfaces using a lattice of rectilinear vortex rings. Perhaps the most comprehensive modern description of the UVLM is given by Katz and Plotkin,[1] however this text, and the literature as a whole, lack a thorough discussion of induced drag calculations. Accurate prediction of unsteady induced drag is of great importance in flexible aircraft flight dynamics[2] and flapping flight applications[3] in which all components of the aerodynamic forces play an important role. The main difficulty associated with induced drag calculations in lifting-surface methods, such as the UVLM and Doublet Lattice Method (DLM)[a], is the inclusion

[a]We refer to the linearised frequency-domain formulation commonly used in aeroelasticity.[4] Since the velocity induced by a constant strength doublet panel is the same as that induced by a vortex ring of the same

of leading-edge suction effects.

The simplest example of a solution to the leading-edge suction problem comes from thin-aerofoil theory. In the steady case the component of pressure force in the free-stream direction is cancelled by the leading-edge suction force; the drag is therefore zero – D'Alembert's paradox. However, in the unsteady case there may be drag, or thrust, depending on the details of the unsteady motion. Garrick[5] introduced a closed-form solution for the propulsion of a sinusoidally oscillating aerofoil by considering the suction force due to the contribution of infinite, but integrable, vorticity at an infinitely-small, rounded leading-edge.[6] The sectional drag has the form

$$d = \alpha l - \pi \rho_\infty S^2, \tag{1}$$

where S is the leading-edge suction term, which for harmonic plunging and pitching motions is[5]

$$S = \sqrt{\frac{b}{2}} \left[2C(k) \left(U_\infty \alpha + \dot{h} + b \left(\frac{1}{2} - a \right) \dot{\alpha} \right) - b\dot{\alpha} \right], \tag{2}$$

where $C(k) = F(k) + iG(k)$ is Theodorsen's function.[7] This term arises from downwash at the leading-edge induced by the bound vorticity, and wake vorticity, relative to the unsteady motion of the aerofoil.

An equivalent approach in three dimensions is found in solutions built by superposition of horseshoe vortices, such as the Unsteady Lifting-Line Method.[8] The unsteady force contribution from an incremental segment of vorticity, described by vector $\delta\mathbf{l}$ orientated in the spanwise wing direction along the quarter-chord, is calculated using the unsteady vector form of the Joukowski theorem yielding $\delta\mathbf{F} = \delta\mathbf{F}_{st} + \delta\mathbf{F}_{unst}$, where

$$\delta\mathbf{F}_{st} = \rho_\infty \Gamma \left(\mathbf{U} \times \delta\mathbf{l} \right), \tag{3}$$

and

$$\delta\mathbf{F}_{unst} = \rho_\infty \frac{\partial \Gamma}{\partial t} c \left(\hat{\mathbf{U}} \times \delta\mathbf{l} \right). \tag{4}$$

In the above equations Γ is the circulation around an incremental vortex segment of length $\delta\mathbf{l}$, and $\mathbf{U}$ is the local flow velocity which is assumed normal to $\delta\mathbf{l}$. The unit vector $\hat{\mathbf{U}} = \mathbf{U}/|\mathbf{U}|$ describes the direction of the local flow velocity. The force component in the free-stream direction is referred to as induced drag.

This approach has been extended to the UVLM,[1,9] although the resulting methods have not been discussed thoroughly, or compared. Therefore, this technical note seeks to present and compare the two force calculation methods currently used in the UVLM in which induced

shape and strength,[1] vortex and doublet lattices are actually equivalent. However, the UVLM is typically formulated in the time domain with the non-penetration boundary condition enforced on the instantaneous deformed surface geometry.

drag is predicted including leading-edge suction effects. For validation purposes a comparison with analytical solutions[5,7] to limit cases is first presented. Following this the convergence of both methods is investigated for a finite wing application; firstly for a steady-state case, and then for a series of related unsteady cases of increasing reduced frequency.

II. Method

Capturing leading-edge suction effects in the UVLM requires that force contributions from all bound singularities are included. The force from each of the ring segments is given by Eq. (3) and is quasi-steady in nature. The unsteady contribution presented in Eq. (4) is a force originating from the unsteady part of Bernoulli's equation that, in the absence of a surface, is approximated to act in the direction $\hat{\mathbf{U}} \times \delta\mathbf{l}$. Since the UVLM resolves the mean aerodynamic surface the unsteady force component from Bernoulli's equation can be orientated, as intended, along the normal of each vortex ring (panel).[9] This leads to an unsteady contribution from each panel

$$\mathbf{F}_{ij} = \rho_\infty \frac{\partial \Gamma_{ij}}{\partial t} A_{ij} \mathbf{n}_{ij}, \tag{5}$$

where A_{ij} is the panel area, $\mathbf{n}_{ij}$ is the panel normal vector, and i and j are panel indices in the chordwise and spanwise directions respectively. Therefore the force on each vortex ring is obtained by adding the steady contribution from each of its vortex segments (3) to the unsteady component from the panel (5). For the proceeding discussion, this method will be referred to as the *Joukowski method*.

A second force calculation method is given by Katz & Plotkin.[1] The unsteady Bernoulli equation is applied to the top and bottom surfaces of each panel in order to find the pressure jump, which results in a local lift contribution

$$\begin{aligned} L_{ij}^{local} \;=\; \rho_\infty \Bigg(& \left(\mathbf{U}_{ij}^m + \mathbf{U}_{ij}^w\right) . \boldsymbol{\tau}_{ij}^c \; \frac{\Gamma_{ij} \;-\; \Gamma_{i-1,j}}{\Delta c_{ij}} \\ & + \;\; \left(\mathbf{U}_{ij}^m + \mathbf{U}_{ij}^w\right) . \boldsymbol{\tau}_{ij}^s \; \frac{\Gamma_{ij} \;-\; \Gamma_{i,j-1}}{\Delta b_{ij}} \;\; + \;\; \frac{\partial \Gamma_{ij}}{\partial t} \Bigg) A_{ij} \cos\alpha_{ij}, \end{aligned} \tag{6}$$

where $\mathbf{U}_{ij}^m$ and $\mathbf{U}_{ij}^w$ are velocity contributions from the surface motion (relative inertial velocity) and the wake vorticity respectively, at the panel collocation point. The contribution of bound vorticity is approximated by two components arising from the gradient of circulation along the direction of panel tangential vectors $\boldsymbol{\tau}_{ij}^c$ and $\boldsymbol{\tau}_{ij}^s$, in the chordwise and spanwise directions respectively. Katz & Plotkin[1] note that the force resulting from the pressure jump does not include leading-edge suction effects and is only adequate for lift pre-

diction. Hence, the local angle of attack α_{ij} has been introduced, which for general motions is $\alpha_{ij} = \tan^{-1}\left(\mathbf{U}^m_{ij}.\mathbf{n}_{ij} \;/\; \mathbf{U}^m_{ij}.\boldsymbol{\tau}^c_{ij}\right)$.[3] Note that Eq. (6) does not account for sideslip.

The induced drag is then calculated using the component of downwash that acts along the local lift vector. The local lift vector is found by linear transformation of the panel normal vector to a plane perpendicular to the relative inertial velocity, which is achieved using an orthogonal projection operator,[10] $P_{\hat{\mathbf{U}}^m_{ij}} = I - \hat{\mathbf{U}}^m_{ij}\ \hat{\mathbf{U}}^{m\intercal}_{ij}$, where I is the identity matrix. The local drag is then

$$D^{local}_{ij} = \rho_\infty \left[-\left(\mathbf{U}^{bc}_{ij} + \mathbf{U}^w_{ij}\right) . \left(P_{\hat{\mathbf{U}}^m_{ij}}\mathbf{n}_{ij}\right) \left(\Gamma_{ij} \;-\; \Gamma_{i-1,j}\right) \Delta b_{ij} \;+\; \frac{\partial \Gamma_{ij}}{\partial t} A_{ij} \sin\alpha_{ij} \right], \qquad (7)$$

where the superscript bc indicates a velocity is calculated considering bound, chordwise-orientated vorticity only. At the leading-edge $\Gamma_{i-1,j}$ is set to zero. The total force contribution from each panel is then, $\mathbf{F}_{ij} = D^{local}_{ij}\hat{\mathbf{U}}^m_{ij} + L^{local}_{ij} P_{\hat{\mathbf{U}}^m_{ij}}\mathbf{n}_{ij}$.

In addition to its complexity for general motions, this approach also has the drawback that the drag is approximated based on velocities calculated at the collocation points, not directly on the vortex segments, introducing additional discretisation error. Also, only chordwise-orientated vorticity contributes to the local drag term. In contrast, in the Joukoswki Method the velocity is calculated at the midpoint of every vortex segment. For a given discretisation, the Joukowski method carries a slight computational overhead compared to that of Katz and Plotkin,[1] but it is easier to implement for general cases with complex kinematics.

III. Results

What follows is a comparison of the force calculation methods described above. Results are also benchmarked against the analytical solutions of Theodorsen[7] and Garrick.[5] Garrick's work is useful for drag benchmarking yet it is very rare to find results for pitching motions presented as a function of time – usually expressions for periodically time-averaged coefficients are presented.[11,12] In order to adapt the general 3D implementation of the UVLM into a 2D problem a single rectangular surface was modelled with an extremely large aspect ratio, $\mathcal{O}(10^3)$. Following the comparison with 2D analytical solutions, results are presented from steady and unsteady simulations of a finite-wing in order to highlight differences in the convergence of the methods for 3D problems.

A. Plunging and Pitching Aerofoils

The simulations here are of flat-plates exhibiting small-amplitude oscillations with fully-developed linear wakes. For harmonic plunging motions, $h = -\bar{h}\cos(ks)$, Garrick's solution

can be written in non-dimensional form as[13]

$$C_d(s) \;=\; -2\pi k^2 \frac{\bar{h}^2}{b^2}\left[G\left(k\right)\cos\left(ks\right) \;+\; F\left(k\right)\sin\left(ks\right)\right]^2, \tag{8}$$

where the sectional drag coefficient, C_d, is presented as a function of non-dimensional time, $s = \frac{U_\infty t}{b}$. The reduced frequency is defined as $k = \frac{\omega b}{U_\infty}$. Inspection of Eq. (8) reveals that there is a propulsive force for plunging motions at all reduced frequencies that is proportional to both the square of the reduced frequency and the square of the plunging amplitude.

For pitching, an additional parameter defines the centre of rotation, a, which is non-dimensionalised by the semi-chord and measured from the mid-chord as positive in the aft direction. The induced drag is then given by Eq. (1), which in non-dimensional form is

$$C_d(s) = \alpha C_l(s) - C_s(s), \tag{9}$$

where the suction force and lift coefficients, for pitching motions of the type $\alpha = \bar{\alpha}\sin(ks)$, are, respectively,

$$C_s(s) = \frac{\pi\bar{\alpha}^2}{2}\left[\Upsilon_1\sin(ks) + \Upsilon_2\cos(ks)\right]^2, \tag{10}$$

and

$$\begin{aligned} C_l(s) = \pi\bar{\alpha}\Big[&k\cos(ks) + ak^2\sin(ks) \\ &+ 2F(k)\left(\sin(ks) + \left(\frac{1}{2}-a\right)k\cos(ks)\right) \\ &+ 2G(k)\left(\cos(ks) - \left(\frac{1}{2}-a\right)k\sin(ks)\right)\Big], \end{aligned} \tag{11}$$

where $\Upsilon_1 = 2\left[F(k) - kG(k)\left(\frac{1}{2}-a\right)\right]$, and $\Upsilon_2 = 2\left[G(k) + kF(k)\left(\frac{1}{2}-a\right)\right] - k$. The results of Eqs. (8) & (9) are compared to results computed with the UVLM in Fig. 1, where phase plots of induced drag against kinematics are shown for a given discretisation at two reduced frequencies. The agreement between the UVLM results and the linear theory is good with the exception of the Katz & Plotkin method for $k = 1$ plunging (Fig. 1(b)) which requires a finer mesh for convergence.

This is investigated further through a convergence exercise on both force calculation methods with respect to the chordwise discretisation. The results for both plunging and pitching motions can be found in Fig. 2, where the error is defined as

$$error \;=\; \frac{\mathrm{RMS}\left(C_{d_{UVLM}} - C_{d_{Garrick}}\right)}{\max\limits_t \left|C_{d_{Garrick}}\right|}, \tag{12}$$

where the maximum of the modulus is used in the denominator to avoid issues arising when

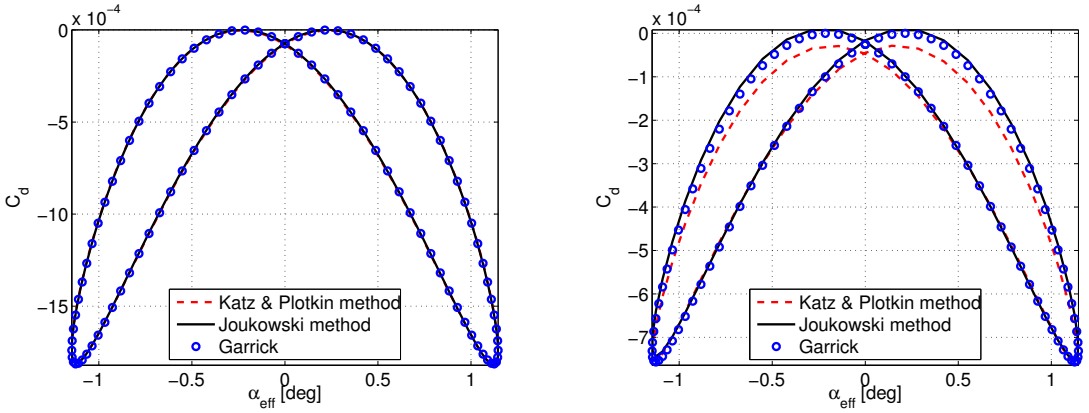

(a) Plunging at $k = 0.1$

(b) Plunging at $k = 1$

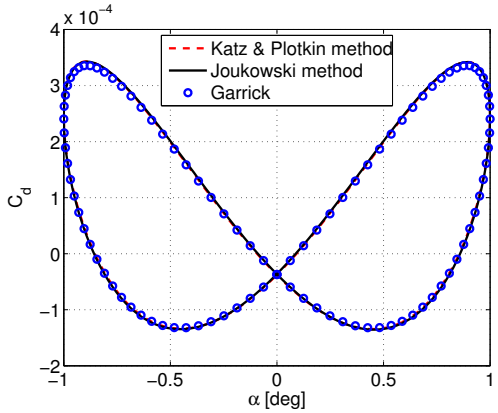

(c) Pitching at $k = 0.1$

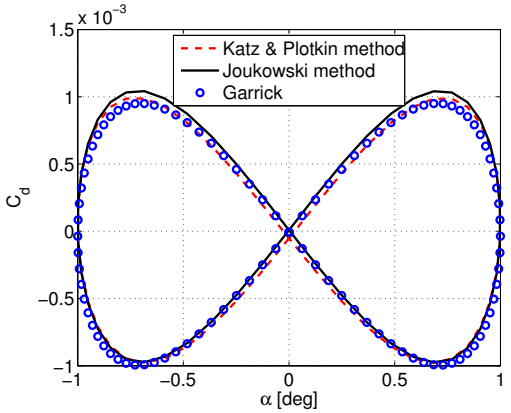

(d) Pitching at $k = 1$

Figure 1. *Unsteady induced drag for sinusoidal oscillations in plunge and pitch. In plunge* $\alpha_{eff} = \tan^{-1}\left(k\frac{\bar{h}}{b}\sin(ks)\right)$ *with* $\frac{\bar{h}}{b} = 0.2$ *at* $k = 0.1$*, and* $\frac{\bar{h}}{b} = 0.02$ *at* $k = 1$*. In pitch* $\bar{\alpha} = 1\,\text{deg}$*, and* $a = -0.5$*.* $M = 16$ *and* $\frac{\Delta t\ U_\infty}{c} = \frac{1}{16}$ *in all cases.*

calculating the relative error as $C_{d_{Garrick}}$ approaches zero. When prescribing the time step in the UVLM it is useful to define a non-dimensional time step, $\frac{\Delta t\ U_\infty}{c}$. From this definition, and assuming that the chord is split into M equally-sized panels, the time step can be set as $\frac{\Delta t\ U_\infty}{c} = \frac{1}{M}$ to ensure trailing-edge and newly-shed wake panels have the same area.

The convergence of both methods for plunging oscillations at $k = 0.1$ is shown in Fig. 2(a). In this case the convergence is very fast, with errors less than 1% for all discretisations shown. For higher reduced frequencies the convergence pattern is similar, with the Joukowski method converging marginally faster than the Katz and Plotkin method (Fig. 2(b)). Convergence is also shown for pitching oscillations at $k = 0.1$ in Fig. 2(a) using the same error metric, Eq. (12). Convergence of the Katz & Plotkin method and the Joukowski method are similar in this case. Interestingly, at $k = 1$ the Katz & Plotkin method shows slightly better convergence (Fig. 2(b)) for pitching oscillations. This may be because this

method uses velocities at the collocation point, and hence gives a better approximation of the tangential velocities when there are linear variations of relative inertial velocity across the panel. Finally, increased spatial resolution is required at higher reduced frequencies for both pitch and plunge motions. Therefore, for a given discretisation, both methods show increasing discrepancies with the analytical theory as the frequency increases.

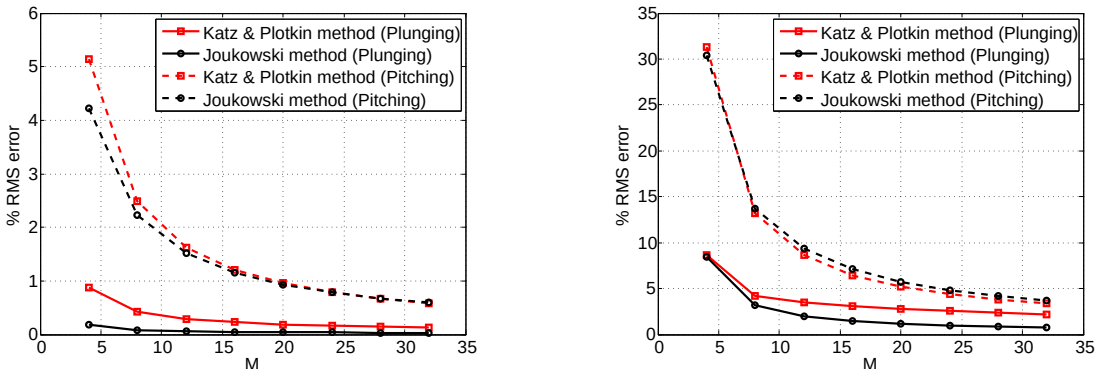

(a) $k = 0.1$ (b) $k = 1$

Figure 2. *RMS error in drag as a function of M, the number of chordwise panels. Plunging motion with* $\frac{\bar{h}}{b} = 0.2$ *at* $k = 0.1$*, and* $\frac{\bar{h}}{b} = 0.02$ *at* $k = 1$*. Pitching motion with* $\bar{\alpha} = 1\,\text{deg}$*, and* $a = -0.5$*.* $\frac{\Delta t\, U_\infty}{c} = \frac{1}{M}$ *in all cases.*

B. Pitching of a Finite-Wing

A low aspect-ratio finite wing (AR = 4) is simulated with the UVLM to further investigate the convergence of both force calculation methods. The steady results, at a constant angle of attack, are shown alongside results from pitching oscillations about the quarter-chord at different reduced frequencies (Fig. 3) in order to ascertain any additional effect that reduced frequency may have on convergence. The error has been normalized with respect to the Joukowski method result from the most densely panelled simulation at each frequency.

There are three length scales in the oscillation of a finite wing:[14] chord, c; span, B; and the wake wavelength, $\lambda = \frac{\pi c}{k}$. Analysis of a low-aspect-ratio wing ($B \approx c$) is a highly three-dimensional problem, and care must be taken to discretise the wing appropriately in both the spanwise and chordwise directions. The steady result (at $k = 0$) where $\lambda \to \infty$, shows the convergence of the Katz & Plotkin method is far slower than the Joukowski method for such a problem. This is almost certainly due to the discretisation error incurred by calculating downwash at the collocation points. In the case of a high reduced frequency (i.e when $\lambda \approx c$) the problem becomes more two-dimensional.[14] This effect is observed in the results of Fig. 3 as the coalescence of error curves with increasing reduced frequency.

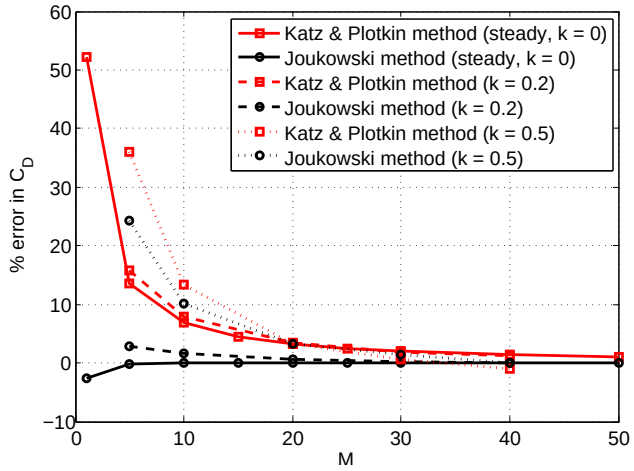

Figure 3. *Convergence of steady drag, and unsteady mean drag, with respect to chordwise panelling for a flat-plate of aspect-ratio 4. Results for* $\alpha = 5^o \cos(ks)$, $\frac{\Delta t\, U_\infty}{c} = \frac{1}{M}$, *and* $N = 50$.

IV. Conclusion

Unsteady aerodynamics methods that use lifting-surface approximations require solution of the leading-edge suction in their induced drag calculations. Results of two force calculation methods used in the UVLM, the *Joukowski method* and the *Katz & Plotkin method*, have been presented with a focus on the calculation of unsteady induced drag. Comparisons of both methods have been made with analytical solutions for the induced drag of plunging and pitching flat-plate aerofoils. It was shown that the methods converge equally well to the analytical solutions as finer discretisations are used.

A 3D problem was also investigated to highlight convergence properties of the methods with respect to chordwise panelling. For the low-aspect-ratio wing investigated the steady drag was found to converge very slowly using the Katz & Plotkin method, whereas the Joukowski method exhibited very fast convergence. This is attributed to the discretisation error in the Katz & Plotkin method associated with evaluating velocities at panel collocation points, rather than on vortex segments. It is known that if the reduced frequency of the wing motion is very high the problem becomes locally two-dimensional, and this effect was observed in the results presented here as the coalescence of error curves with increasing reduced frequency. At moderate-to-low reduced frequencies the Joukowksi method was found to offer the same level of accuracy for a much coarser discretisation and therefore presents itself as a desirable option for 3D applications, such as the flight dynamics of very flexible aircraft.

Acknowledgments

The authors would like to thank Professor Mike Graham of Imperial College London for his part in numerous useful and enlightening discussions. This work was supported by the EPSRC of the United Kingdom under grant number EP/I014683/1.

References

[1]Katz, J. and Plotkin, A., *Low-Speed Aerodynamics*, Cambridge University Press, 2001.

[2]Palacios, R., Murua, J., and Cook, R., "Structural and aerodynamic models in nonlinear flight dynamics of very flexible aircraft," *AIAA Journal*, Vol. 48, No. 11, 2010, pp. 2648 – 2659.

[3]Stanford, B. K. and Beran, P. S., "Analytical Sensitivity Analysis of an Unsteady Vortex-Lattice Method for Flapping-Wing Optimization," *Journal of Aircraft*, Vol. 47, No. 2, 2010, pp. 647 – 662.

[4]Albano, E. and Rodden, W., "A doublet-lattice method for calculating lift distributions on oscillating surfaces in subsonic flows." *AIAA Journal*, Vol. 7, No. 2, 1969, pp. 279 – 285.

[5]Garrick, I. E., "Propulsion of a flapping and oscillating airfoil," NACA Report 567, National Advisory Committee for Aeronautics, 1937.

[6]von Karman, T. and Burgers, J., *General Aerodynamic Theory - Perfect Fluids: Aerodynamic Theory. Vol. 2, edited by W. Durand*, Dover, New York, 1968.

[7]Theodorsen, T., "General theory of aerodynamic instability and the mechanism of flutter," NACA Report 496, National Advisory Committee for Aeronautics, 1935.

[8]Drela, M., "Integrated simulation model for preliminary aerodynamic, structural, and control-law design of aircraft," *40th AIAA/ASME/ASCE/AHS/ASC Structures, Structural Dynamics and Materials (SDM) Conference*, St. Louis, MO, April 1999.

[9]Pesmajoglou, S. D. and Graham, J. M. R., "Prediction of aerodynamic forces on horizontal axis wind turbines in free yaw and turbulence," *Journal of Wind Engineering and Industrial Aerodynamics*, Vol. 86, No. 1, 2000, pp. 1 – 14.

[10]Geradin, M. and Cardona, A., *Flexible Multibody Dynamics: A Finite Element Approach*, John Wiley, 2001.

[11]Garrick, I. E., *Nonsteady Wing Characteristics, Division F., Vol. VII High Speed Aerodynamics and Jet Propulsion; Aerodynamic Components of Aircraft at High Speeds, Eds. Donovan, AF and Lawrence, HR*, Princeton University Press, Princeton, NJ, 1957.

[12]Jones, K. D. and Platzer, M. F., "Numerical computation of flapping-wing propulsion and power extraction," *35th AIAA Aerospace Sciences Meeting and Exhibit*, Reno, NV, Jan. 1997.

[13]Gulcat, U., "Propulsive force of a flexible flapping thin airfoil," *Journal of Aircraft*, Vol. 46, No. 2, 2009, pp. 465 – 473.

[14]Ahmadi, A. R. and Widnall, S. E., "Unsteady lifting-line theory as a singular perturbation problem," *Journal of Fluid Mechanics*, Vol. 153, No. 1, 1985, pp. 59 – 81.